Molecular Therapy
Original Article

On- and off-target effects of paired CRISPR-Cas nickase in primary human cells

Julia Klermund,[1,2] Manuel Rhiel,[1,2] Thomas Kocher,[3] Kay Ole Chmielewski,[1,2,4] Johannes Bischof,[3] Geoffroy Andrieux,[5,6] Melina el Gaz,[1,2] Stefan Hainzl,[3] Melanie Boerries,[5,6,7] Tatjana I. Cornu,[1,2,6] Ulrich Koller,[3] and Toni Cathomen[1,2,6]

[1]Institute for Transfusion Medicine and Gene Therapy, Medical Center – University of Freiburg, 79106 Freiburg, Germany; [2]Center for Chronic Immunodeficiency (CCI), Medical Center – University of Freiburg, 79106 Freiburg, Germany; [3]EB House Austria, Research Program for Molecular Therapy of Genodermatoses, Department of Dermatology and Allergology, University Hospital of the Paracelsus Medical University Salzburg, 5020 Salzburg, Austria; [4]PhD Program, Faculty of Biology, University of Freiburg, 79104 Freiburg, Germany; [5]Institute of Medical Bioinformatics and Systems Medicine, Medical Center – University of Freiburg, 79110 Freiburg, Germany; [6]Faculty of Medicine, University of Freiburg, 79110 Freiburg, Germany; [7]German Cancer Consortium (DKTK) and German Cancer Research Center (DKFZ), Partner Site Freiburg, 79106 Freiburg, Germany

Undesired on- and off-target effects of CRISPR-Cas nucleases remain a challenge in genome editing. While the use of Cas9 nickases has been shown to minimize off-target mutagenesis, their use in therapeutic genome editing has been hampered by a lack of efficacy. To overcome this limitation, we and others have developed double-nickase-based strategies to generate staggered DNA double-strand breaks to mediate gene disruption or gene correction with high efficiency. However, the impact of paired single-strand nicks on genome integrity has remained largely unexplored. Here, we developed a novel CAST-seq pipeline, dual CAST, to characterize chromosomal aberrations induced by paired CRISPR-Cas9 nickases at three different loci in primary keratinocytes derived from patients with epidermolysis bullosa. While targeting *COL7A1*, *COL17A1*, or *LAMA3* with Cas9 nucleases caused previously undescribed chromosomal rearrangements, no chromosomal translocations were detected following paired-nickase editing. While the double-nicking strategy induced large deletions/inversions within a 10 kb region surrounding the target sites at all three loci, similar to the nucleases, the chromosomal on-target aberrations were qualitatively different and included a high proportion of insertions. Taken together, our data indicate that double-nickase approaches combine efficient editing with greatly reduced off-target effects but still leave substantial chromosomal aberrations at on-target sites.

INTRODUCTION

Targeted genome editing using designer nucleases has been successfully employed in clinical trials to treat various inherited genetic disorders.[1–3] The CRISPR-Cas system, comprising a Cas nuclease and a chimeric single-guide RNA (gRNA), is particularly favored for its high efficiency, versatility, and ease of introducing precise DNA double-strand breaks (DSBs). The prototypic *Streptococcus pyogenes* (Sp) Cas9 system—the most commonly used CRISPR-Cas platform—recognizes the target site through a 20 nt protospacer sequence specified by the gRNA and a short 5′-NRG protospacer-adjacent motif (PAM).[4,5] Few mismatches between the guide and target sequence can be tolerated, enabling unintended cleavage at off-target sites.[6,7] DSBs at on- and off-target sites are primarily repaired by non-homologous end joining (NHEJ), which can lead to small insertions and deletions (indels) at the break site.[8] Alternative (alt)-NHEJ pathways, such as DNA polymerase theta (Pol θ)-mediated end joining (TMEJ), contribute to mutagenic repair of the DSBs.[9,10] In S-G2 phase, error-free DSB repair is enabled by the homology-directed repair (HDR) pathway, which can be harnessed in therapeutic genome editing by providing a DNA repair template that shares homology with the target site.[11,12]

To assess the safety of genome editing, off-target analyses test the specificity of a particular Cas9-gRNA ribonucleoprotein (RNP) complex. *In silico* tools such as Cas-OFFinder,[13] COSMID,[14] and CRISPRme[15] predict potential off-target sites based on sequence similarity to the protospacer. Experimental methods include *in vitro* assays, such as CIRCLE-seq and CHANGE-seq,[16,17] or cell-based assays, such as GUIDE-seq[18] and DISCOVER-seq.[19] Importantly, besides indel formation at on- and off-target sites, chromosomal aberrations are well-known genotoxic side effects of CRISPR-Cas9 editing. They include large deletions,[20–22] inversions,[22,23] translocations,[22–25] chromosomal truncations,[26,27] loss of heterozygosity,[28] loss of imprinting,[28] and chromothripsis.[29] Methods to detect such chromosomal aberrations include LAM-HTGTS,[24,25] PEM-seq,[30,31]

Received 30 August 2023; accepted 5 March 2024;
https://doi.org/10.1016/j.ymthe.2024.03.006.

Correspondence: Toni Cathomen, Institute for Transfusion Medicine and Gene Therapy, Medical Center – University of Freiburg, 79106 Freiburg, Germany.
E-mail: toni.cathomen@uniklinik-freiburg.de

and our recently described CAST-seq.[22,23] CAST-seq is not only able to detect large deletions and inversions at the on-target site as well as intra- and inter-chromosomal translocations but also to nominate off-target sites.

When guided to a specific locus, the Cas9 nuclease uses its two cleavage domains, HNH and RuvC, to induce a blunt-ended DSB.[4,5] A D10A mutation in the RuvC domain creates a Cas9 nickase (Cas9n) enzyme that only cleaves the strand complementary to the gRNA, creating a single-strand break (SSB), also termed a "nick."[32] Guiding two Cas9n RNPs to opposite strands in close proximity leads to a paired nick, causing a staggered DSB.[33,34] Efficient DSB induction, evidenced by significant indel formation, occurs between the nicks if they are offset by up to 100 bp.[34] Consequently, off-target sites of the respective nickases are only exposed to a single nick, which is repaired by the high-fidelity base excision repair (BER) pathway.[35] This critically lowers the genotoxic potential of paired-nickase-based approaches compared to a DSB-inducing agent. Nonetheless, during S phase of the cell cycle, an SSB can be converted to a DSB if the replication fork stalls and collapses at the nick site,[36] leading to low levels of indel formation.[37,38]

Several studies in human cells have shown that indel formation at known off-target sites is reduced or absent when employing nickase approaches as opposed to CRISPR-Cas9 nuclease-based editing.[34,38–41] Moreover, chromosomal aberrations were reduced below the limit of detection when using single-nickase editing.[26,37,42] Furthermore, in cells edited with paired CRISPR-Cas9 nickases, translocations between the target site and known off-target sites could not be detected by qualitative translocation PCR.[38] However, a systematic genome-wide and sensitive analysis of on- and off-target aberrations in double-nickase-edited primary human cells is lacking.

To address this matter, we compared side by side the chromosomal aberrations induced by Cas9 nucleases or nickases in primary keratinocytes derived from patients with epidermolysis bullosa (EB). EB comprises a group of rare genetic disorders characterized by impaired skin function due to mutations in various genes. Recessive dystrophic EB (RDEB) is caused by mutations in the *COL7A1* gene, while junctional EB (JEB) can be caused by alterations in the *COL17A1* or *LAMA3* loci.[43] Pre-clinical research has aimed to correct these mutations using CRISPR-Cas nuclease and double-nickase approaches. In RDEB keratinocytes, a double-nickase approach combined with single-stranded oligodeoxynucleotides (ssODNs) achieved a correction of up to 21% of *COL7A1* alleles using HDR.[41,44] Similarly, paired Cas9n or Cas9 nuclease approaches have been used to efficiently correct *COL17A1* mutations through NHEJ reframing or HDR.[40,45]

In order to analyze the induction of gross chromosomal aberrations resulting from Cas9 double-nickase editing, we designed a novel CAST-seq pipeline, termed dual (D)-CAST. D-CAST is a further development of T-CAST,[23] an algorithm that was developed to evaluate TALEN-edited samples. Analyzing EB patient-derived keratinocytes edited at the loci *COL7A1*, *COL17A1*, or *LAMA3*, we identified chromosomal rearrangements only in Cas9-nuclease-edited cells and confirmed mutagenic DNA repair at these previously unknown off-target sites using targeted amplicon sequencing. Our analyses underscore the high specificity and sensitivity of the D-CAST pipeline in detecting off-target-mediated translocations (OMTs) from sites that harbor indels at a frequency as low as 0.47%. No translocations could be detected after single- or paired-nickase editing for any of the loci, confirming the good safety profiles of these strategies. Conversely, D-CAST revealed that chromosomal aberrations at the on-target site, such as large deletions, were prominent in double-nickase-edited cells, representing an unwanted editing outcome that was independently confirmed by long-read sequencing.

RESULTS

Double-nickase-based genome editing prevents chromosomal translocations

To test in a genome-wide manner whether single- or double-nickase editing would lead to translocations with potential off-target sites in clinically relevant cells, we firstly used D-CAST to analyze cells treated with well-characterized, highly efficient SpCas9 (hereafter called Cas9)-based RNPs targeting the *COL7A1* gene located on the p arm of chromosome 3 (Figure 1A). These RNPs have previously been used for an HDR-based correction of the 425A>G mutation in exon 3 of *COL7A1*, causing the severe recessive dystrophic form of RDEB.[41,44] Patient-derived keratinocytes (RDEB223, homozygous c.425A>G) were electroporated with different RNPs: single-nuclease approaches using either Cas9-gRNA1 (g1) or Cas9-gRNA2 (g2) to induce blunt-ended DSBs at the respective target sites, a paired Cas9n approach using Cas9n-g1 and Cas9n-g2 (Cas9n-g1+2) simultaneously to induce a staggered-end DSB, or single-nickase approaches using either Cas9n-g1 or Cas9n-g2 to induce SSBs (Figure 1A). Genomic DNA was extracted after a week and on-target activity determined using next-generation sequencing (NGS)-based amplicon sequencing. The indel frequencies were high for all DSB-inducing conditions at about 98% for Cas9-g1, Cas9-g2, and Cas9n-g1+2 (Figure S1A). As described before,[36,37] significant formation of indels was also detected when inducing SSBs, albeit at substantially lower frequencies of about 0.3%. The presence of indels in these samples likely indicates conversion of SSBs into DSBs at a low level (Figure S1A).

The same genomic DNA was subjected to CAST-seq analyses (schematic workflow shown in Figure S1B) using bait and decoy primers directed at the *COL7A1* target site (Figures S1C and S1D). The sequences that were fused to the on-target site were subsequently mapped to the genome to identify and classify induced chromosomal rearrangements. D-CAST is a further development of the T-CAST bioinformatic pipeline that was recently developed for TALENs, which improved the classification of the identified rearrangements into OMTs, homology-mediated translocations (HMTs), and non-classified break sites (NBSs).[22,23] Importantly, to account for potential off-target editing and subsequent translocations caused by either RNP in the double-nickase approach, the D-CAST pipeline was adapted for concomitant use of two gRNAs (see materials and methods).

Figure 1. Off-target (OT) effects of paired nickases targeting the *COL7A1* locus

(A) Schematic representation of the *COL7A1* locus on chromosome 3. The positions of the two used gRNAs are highlighted in blue, the protospacer-adjacent motif (PAM) in purple, and the cleavage sites by red triangles. Patient-specific mutation c.425A>G is shown in red with an asterisk. (B) Chromosomal rearrangements. Circos plots summarize the CAST-seq results of single-nuclease- or double-nickase-edited cells. Aberrations at the on-target site are indicated in green, while OT-mediated translocations (OMTs) are shown in red. (C) OT sites. Shown are the chromosomal coordinates of the nominated OT sites for Cas9-g1, the number of CAST-seq hits for each OT, and the alignment to the on-target site. (D) OT activity. Listed are the percentages of indels detected at each nominated OT using NGS. Asterisks denote significant indel frequencies compared to the untreated (UT) sample. "D" indicates numbers stemming from DECODR analysis upon Sanger sequencing and "X" marks previously identified OTs.

Previous off-target analyses for these *COL7A1*-targeting nucleases based on *in silico* prediction and an *in vitro* assay detected one prominent off target for Cas9-g1 in chromosome 7.[41] D-CAST identified 17 additional OMTs in the Cas9-g1-edited cells, while no OMTs were detected for any of the other editing approaches (Figures 1B, 1C, and S1E; Table S1). The D-CAST-nominated off-target sites had up

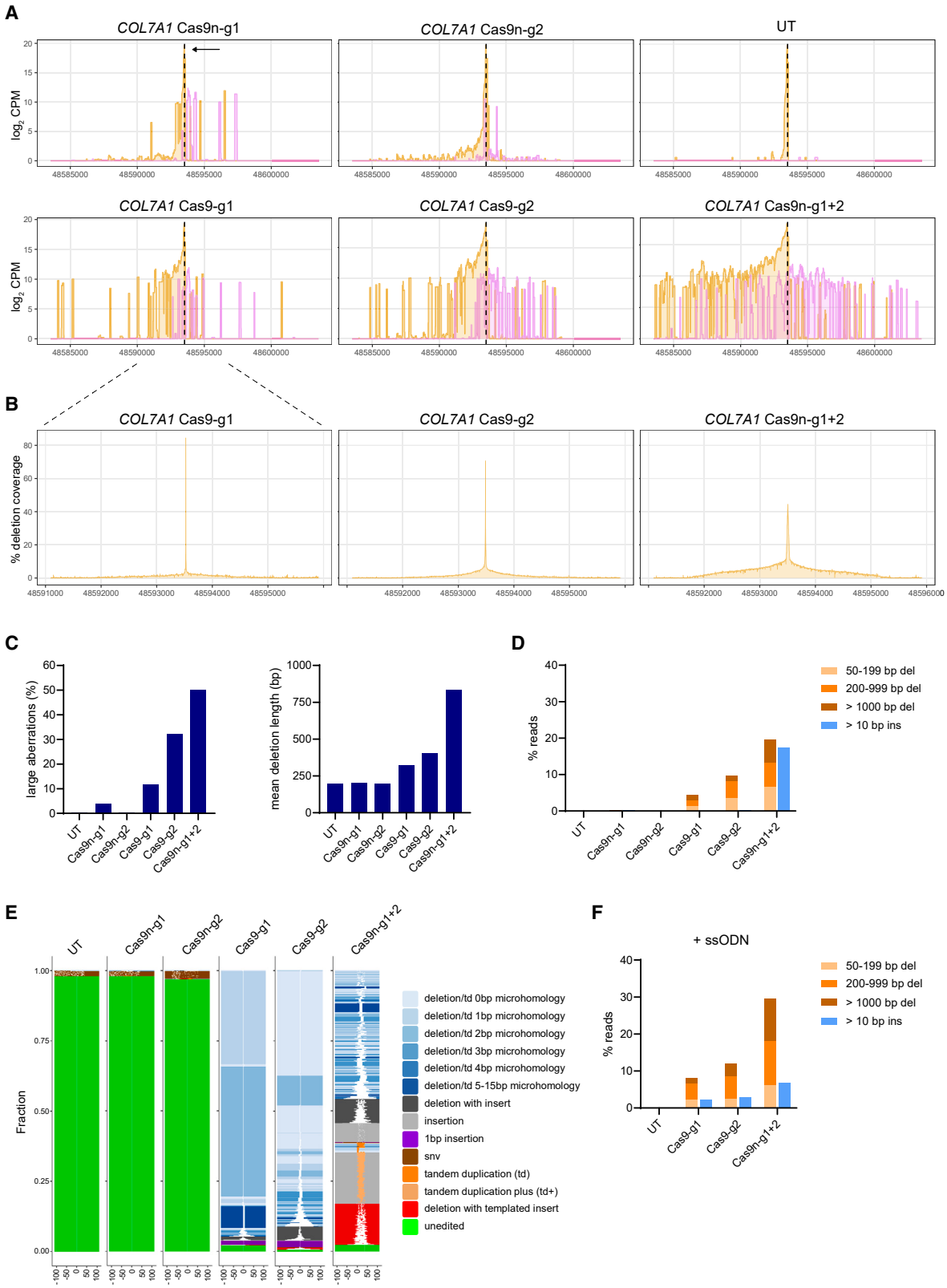

(legend on next page)

to four mismatches in comparison to the *COL7A1* target site (Figure 1C). Targeted amplicon sequencing revealed significant mutagenesis, with up to 93% of alleles carrying indels, at all but one nominated off-target site (Figure 1D). This included the previously identified off target in chromosome 7 (OT4) as well as two *in silico* predicted off-target sites (OT12 and OT14).[41] The remaining 14 off-target sites (i.e., >80% of all off targets) were newly identified by D-CAST. Despite high on-target activity in the double-nickase-edited cells with 97% of edited *COL7A1* alleles, significant indel formation (0.09%) could only be detected at OT4 (Figure 1D). Yet, this low off-target activity did not lead to detectable translocations (Figure 1B). Similarly, single-nickase editing induced indels at OT4 (0.16%), but chromosomal rearrangements were not detected (Figures 1D and S1E; Table S1). In sum, these data confirm that D-CAST is highly sensitive and specific in detecting chromosomal translocations elicited by concomitant on- and off-target activity. Using the novel CAST-seq pipeline that accounts for simultaneous editing with two gRNAs, we show that a paired-nickase approach combines high on-target activity with an improved safety profile when compared to the cognate CRISPR-Cas9 nucleases.

Double-nickase editing induces chromosomal aberrations at the target site

We noticed that the number of CAST-seq hits detected at the *COL7A1* target site were higher in the double-nickase-edited samples as compared to nuclease- or single-nickase-treated samples (Table S1). This high count implied an increased number of large chromosomal aberrations at the on-target site, such as large deletions and inversions. To visualize on-target aberrations, the CAST-seq read coverage within a region of ±10 kb around the *COL7A1* target site was depicted for the different editing approaches (Figure 2A). The coverage plot for the untreated sample exposed a narrow peak at the cleavage position, representing a few cases in which the decoy primer did not prevent on-target amplification or did not bind due to short fragmentation. Visually, large deletions around the on-target site were present in both Cas9-g1- and Cas9-g2-nuclease-edited samples, whereas the single-nickase-edited samples displayed a low frequency of large deletions. The double-nickase-edited cells showed the highest number of large deletions and inversions at the *COL7A1* target site. Of note, CAST-seq only detects large deletions in the sequencing direction.

To confirm the D-CAST results, a 5 kb amplicon spanning the *COL7A1* target site in edited cells was sequenced using Nanopore MinION long-read sequencing. The presence of chromosomal aberrations in Cas9-g2- and Cas9n-g1+2-edited cells could already be inferred from the different lengths of the PCR amplicons encompassing the target site (Figure S2A). When plotting the positions of these deletions for each edited sample, it became evident that the deletion peaks for the Cas9-nuclease-edited samples were high and narrow (Figure 2B), consistent with the analysis of the short-read sequencing demonstrating that the majority of editing outcomes were 1–2 bp deletions at the cut site (Figures S2B and S2C). While the deletion coverage peak was considerably broader for the Cas9n-g1+2 double-nickase sample (Figures 2B and S2C), no deletions were detected in single-nickase-edited samples (Figure S2D).

We next quantified and categorized the CAST-seq-derived read coverage plots and Nanopore-derived deletion coverage plots. For CAST-seq, we calculated both the presence of large (>200 bp) aberrations (deletions and inversions) as a percentage of the total on-target reads as well as the mean deletion length (Figure 2C; calculations in materials and methods). Consistent with the visual representation in the coverage plots, the Cas9n-g1+2 double-nickase samples displayed the highest percentage (up to 50%) of large on-target aberrations compared to 12% and 32% for Cas9-g1 and Cas9-g2 nuclease samples, respectively (Figure 2C). Similarly, the mean deletion length was highest for Cas9n-g1+2 double-nickase samples (Figure 2C). This is in line with the long-read sequencing quantifications where reads containing deletions spanning the on-target site were categorized into (1) intermediate deletions (50–199 bp) and large deletions of (2) 200–999 bp or (3) >1,000 bp (Figure 2D; Table S4). While editing with Cas9-g2 caused more intermediate and large deletions compared to Cas9-g1, double-nickase editing at the *COL7A1* locus led to a ∼2-fold increase in intermediate and large deletions compared to the nucleases (Figure 2D; Table S4). In addition to the deletions, a large number of insertions of >10 bp were detected in a window of 200 bp around the cleavage site for the double-nickase-edited sample only, which likely represents overhang fill in (Figure 2D; Table S4). These observations fit with a more detailed analysis of the *COL7A1* on-target short-read amplicons using the Sequence Interrogation and Quantification (SIQ) PlotteR,[46] which analyzes mutational profiles and classifies repair events. The SIQ PlotteR output confirmed that double-nickase editing led to qualitative differences in DNA repair and led to an increased number of insertions in the form of tandem duplications, i.e., duplications of the sequences adjacent to the cut site, as well as templated insertions (Figure 2E). Altogether,

Figure 2. On-target aberrations at the *COL7A1* locus

(A) Chromosomal aberrations at the on-target site. The CAST-seq coverage plots show all reads mapped to a ±10 kb region around the on-target site. The sequencing direction of the bait primer is indicated by a black arrow. The x axis indicates the chromosomal coordinates, the y axis the log2 read count per million (CPM), and the dotted line the cleavage site. Deletions (DELs) are shown in orange and inversions (INVs) in purple. (B) Long-read sequencing. A 5 kb fragment encompassing the target site was subjected to Nanopore sequencing. The DEL coverage plots indicate the DEL frequency (y axis) per position (x axis). All reads were normalized to the total number of reads per sample, and the values obtained from the UT control were subtracted to decrease sequencing bias. (C) Quantification of CAST-seq coverage. The percentage of large chromosomal aberrations was calculated as the fraction of CAST-seq reads within a ±10 kb window around the cleavage site that were more than 200 bp away from the target site. The mean DEL lengths were calculated within a ±10 kb window around the target site. (D) Quantification of long-read sequencing. Reads of indicated samples were classified into differently sized DELs or insertions. (E) On-target alterations. SIQ PlotteR analysis of the *COL7A1* target site edited with the different indicated RNPs based on NGS-based short-read amplicon sequences. (F) Quantification of long-read sequencing. Reads were classified into differently sized DELs or insertions as in (D), but the indicated samples were edited in the presence of an ssODN (single-stranded oligodeoxynucleotide).

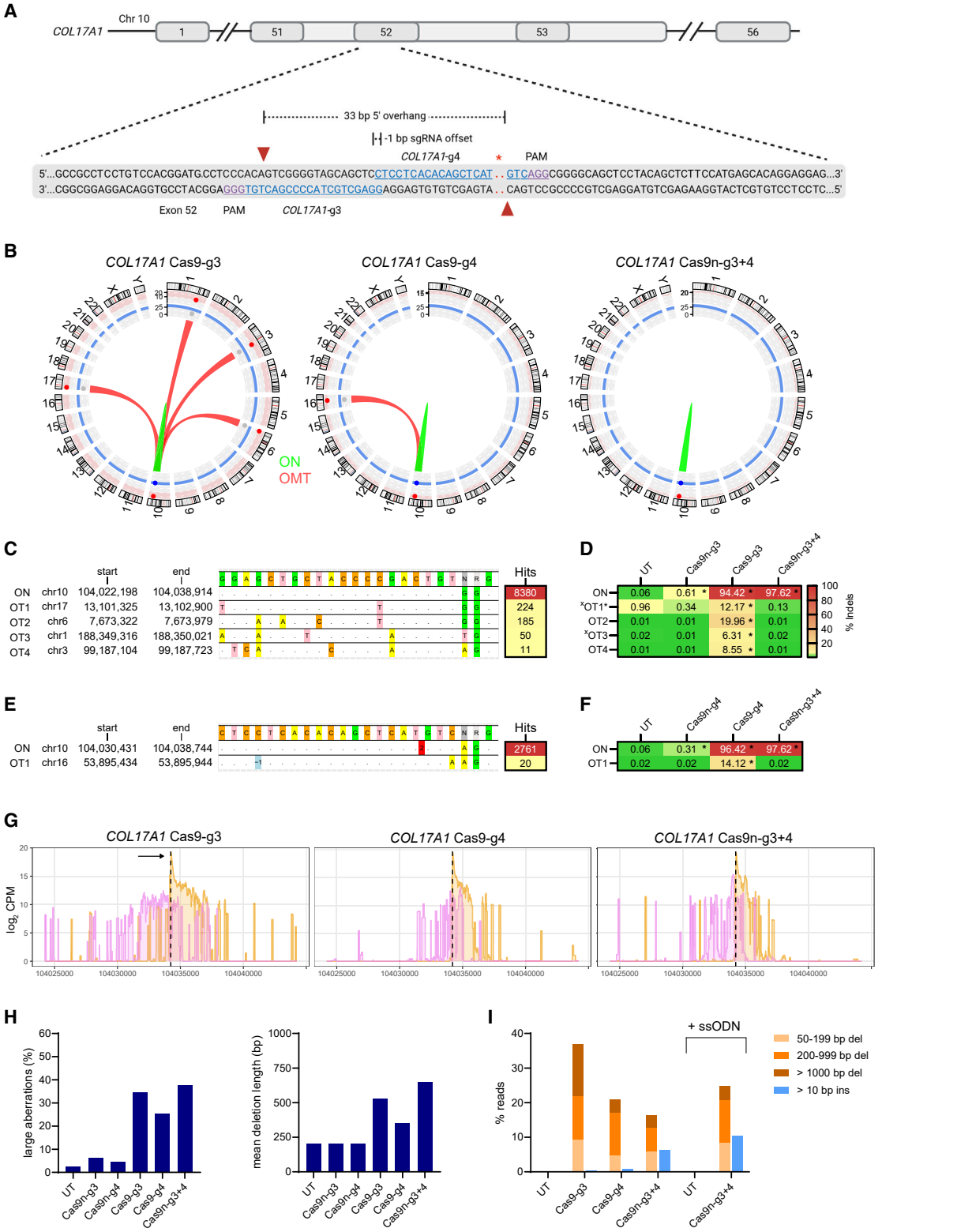

(legend on next page)

double-nickase editing can induce substantial on-target aberrations, which can be directly analyzed by D-CAST.

In order to determine how on-target aberrations may be altered in the presence of a repair template to correct the patient mutation, *COL7A1* editing was repeated in the presence of a 111-bp-long ssODN that contains three nucleotide substitutions: the c.425G>A patient correction and mutations in both PAM sequences (c.426+7C>A, c.426+2G>T; Table S6).[44] The highest correction of the patient mutation (26% of reads) was observed for the dual-nickase-edited samples, whereas only 9.8% and 7.6% of reads contained the corrected patient mutation in the Cas9-g1- and Cas9-2-edited samples, respectively (Table S6). The insertions detected in the single-nuclease-edited samples were, at least partly, due to oligo capturing of the repair template (Figure 2F). More large deletions were detected for the double-nickase-edited samples in the presence of the ssODN, while insertions were reduced (Figures 2F and S2E; Table S4).

Editing at the *COL17A1* locus confirms improved safety of the double-nickase approach

To confirm the finding that double-nickase editing abolishes the emergence of chromosomal translocations seen in nuclease-based editing, a second locus was chosen for CAST-seq analysis. JEB patient-derived keratinocytes (*COL17A1,* homozygous c.3899_3900delCT) were edited with the previously published *COL17A1*-targeting CRISPR-Cas9 nucleases or nickases complexed with gRNAs g3 and g4 (Figure 3A).[40,45] Activity at the *COL17A1* target locus was high for all DSB-inducing conditions, with 94%, 96%, and 97% of edited alleles for Cas9-g3, Cas9-g4, and Cas9n-g3+4, respectively (Figures S3A and S2B). Low but significant formation of indels (0.61% and 0.31% for Cas9n-g3 and Cas9n-g4, respectively) was detected when inducing SSBs (Figure S3B). D-CAST, performed with one decoy primer that prevented amplification of the target site in unedited cells (Figure S3C), revealed four OMTs in Cas9-g3-edited cells, including translocations with two previously identified off-target sites in chromosomes 1 and 17,[40] as well as two newly identified off targets in chromosomes 6 and 3 (Figures 3B and 3C; Table S2). OT4 had five mismatches in comparison to the *COL17A1* target site (Figure 3C). For Cas9-g4-treated cells, one OMT with a novel off-target site in chromosome 16 was detected (Figures 3B and 3E; Table S2). Gross chromosomal aberrations were neither detected in the double-nickase nor in the single-nickase approaches (Figures 3B and S3D; Table S2). NGS-based targeted amplicon sequencing revealed significant indel formation at all CAST-seq-nominated off-target sites in Cas9-g3- (Figure 3D) and Cas9-g4-edited cells (Figure 3F), while none of them were edited over background levels in the paired-nickase- or the respective single-nickase-edited samples. Overall, these data confirm that translocations that are induced by off-target editing in nuclease-treated cells are eliminated when employing double-nickase editing.

CAST-seq coverage plots of the *COL17A1* target region (±10 kb) showed that editing with all DSB-inducing agents (Cas9-g3, Cas9-g4, Cas9n-g3+4) led to a considerable number of large deletions and inversions (Figure 3G). Chromosomal aberrations at the *COL17A1* target site were greatly reduced in the single-nickase-edited samples (Figure S3E). Quantification of the CAST-seq on-target reads at the *COL17A1* locus demonstrated that the percentage of on-target aberrations and the mean deletion length were similar between the single-nuclease and the double-nickase samples (Figure 3H). Long-read Nanopore sequencing of a 5 kb amplicon spanning the *COL17A1* target site showed a higher percentage of long deletions in the Cas9-g3 sample, mainly due to an increased number of very large deletions of >1,000 bp (Figures 3I and S3F; Table S5). This is consistent with the CAST-seq coverage plot of Cas9-g3, which displays the highest spread of reads of all samples (Figure 3G). Again, in the presence of an ssODN repair template to correct the patient mutation[45] (correction efficiency 8.17%; Table S6), the fraction of larger deletions increased in the double-nickase-edited samples (Figures 3I and S3F; Table S5). Analyzing the *COL17A1* short-read on-target amplicons with the SIQ PlotteR confirmed more templated insertions in the double-nickase-edited samples when compared to CRISPR-Cas9-treated samples (Figure S3G).

Establishing a novel paired-nickase strategy for *LAMA3*

Last, a novel double-nickase approach targeted at the *LAMA3* locus, located on the q arm of chromosome 18, was established. Two gRNAs, g5 and g6, were designed, with gRNA g6 being mutation specific (Figure 4A). Upon electroporation of JEB patient-derived keratinocytes (*LAMA3*, homozygous c.466_467delCA) with CRISPR-Cas9 nucleases or nickases, 91%–97% of *LAMA3* alleles were edited for the DSB-inducing conditions (Cas9-g5, Cas9-g6, and Cas9n-g5+6; Figures S4A and S4B). Low but significant formation of indels (0.73% and 0.24% for Cas9n-g5 and Cas9n-g6, respectively) was detected in the single-nickase samples (Figure S4B). Due to the high GC

Figure 3. On-target and OT effects of paired nickases targeting *COL17A1*

(A) Schematic representation of the *COL17A1* locus on chromosome 10. Positions of the two gRNAs are highlighted in blue, the PAM in purple, and the cleavage sites by red triangles. Patient-specific mutation c.3899_3900delCT is shown in red with an asterisk. (B) Chromosomal rearrangements. Circos plots summarize the CAST-seq results of single-nuclease- or double-nickase-edited cells. Aberrations at the on-target site are indicated in green, while OMTs are shown in red. (C–F) OT activity. Shown are the chromosomal coordinates of the nominated OT sites, the number of CAST-seq hits for each OT, and the alignment to the on-target site for Cas9-g3 (C) and Cas9-g4 (E), as well as the fraction of indels detected at each nominated OT using NGS for Cas9-g3 (D) and Cas9-g4 (F). Asterisks indicate significant indel frequencies compared to UT sample. "X" marks previously identified OTs. (G) Chromosomal aberrations at the on-target site. The CAST-seq coverage plots show all reads mapped to a ±10 kb region around the *COL17A1* target site. The sequencing direction of the bait primer is indicated by a black arrow. The x axis indicates the chromosomal coordinates, the y axis the log2 read CPM, and the dotted line the cleavage site. DELs are shown in orange and INVs in purple. (H) Quantification of CAST-seq coverage. The percentage of large chromosomal aberrations was calculated as the fraction of CAST-seq reads within a ±10 kb window around the cleavage site that were more than 200 bp away from the target site. The mean DEL lengths were calculated within a ±10 kb window around the target site. (I) Quantification of long-read sequencing. Reads of indicated samples were classified into differently sized DELs or insertions. ssODN indicates the presence of a repair template.

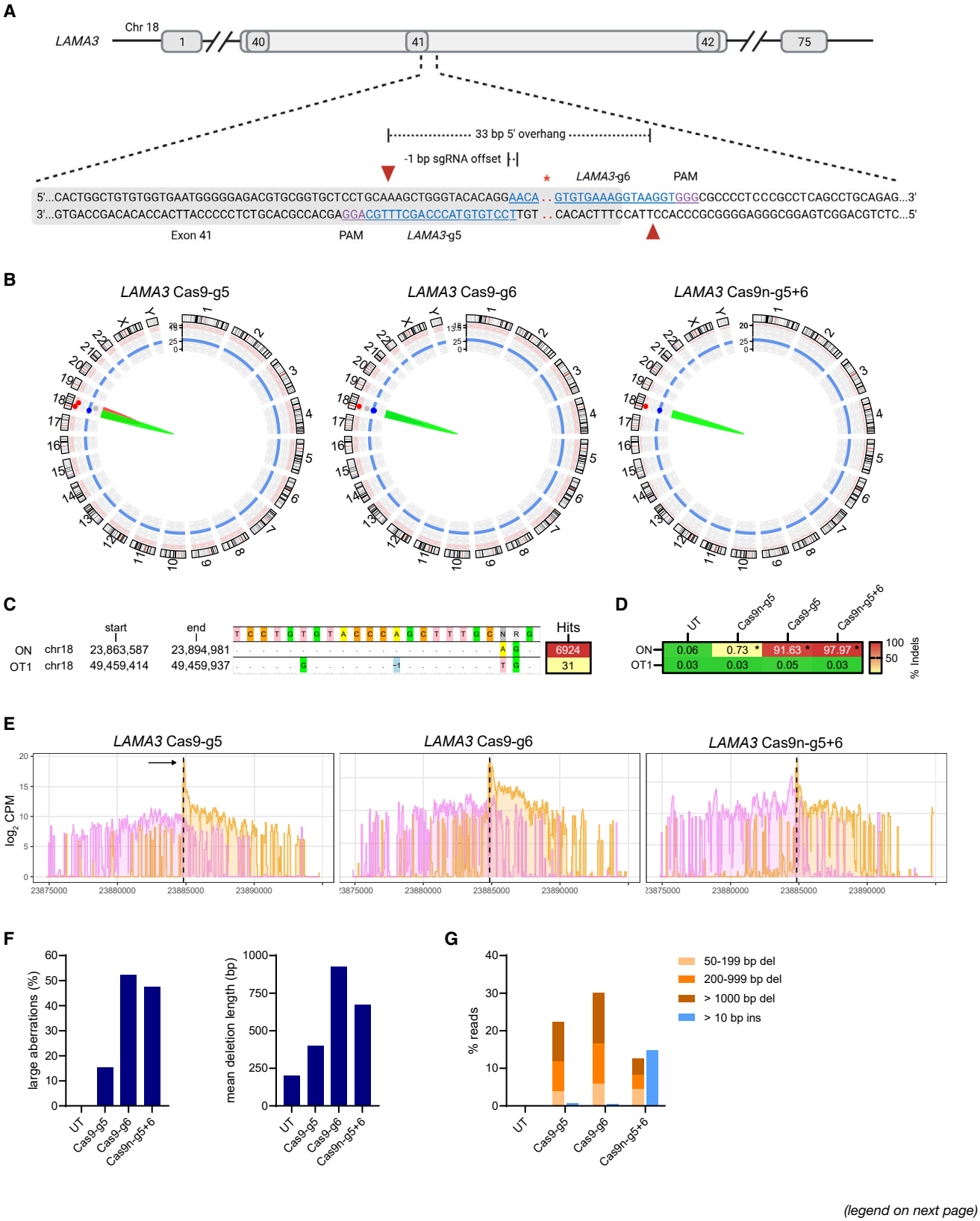

(legend on next page)

content of the *LAMA3* target region, the design of CAST-seq primers was difficult, and different decoy primers were used for the two different target sites (Figures S4A and S4C). In cells edited with Cas9-g5, an OMT event between the *LAMA3* target site and a site located on the same chromosome some 25.5 Mb downstream was detected (Figures 4B; Table S3). Although the nominated off-target site possesses high sequence similarity to the protospacer targeted by gRNA5, with only one mismatch and one bulge (Figures 4C; Table S3), targeted amplicon sequencing did not uncover indel formation (Figure 4D). On the other hand, the 25 Mb chromosomal deletion in the Cas9-g5-edited sample could be verified using a diagnostic PCR involving a forward primer at *LAMA3* and a reverse primer at OT1 (Figure S4D). Sequencing of this PCR amplicon confirmed the presence of a chromosomal rearrangement between *LAMA3* and OT1 with junctions at the two cleavage sites (Figure S4D). No rearrangement could be detected after double-nickase editing (Figures 4B and S4D). The coverage plots encompassing a ±10 kb region around the target sites showed a comparable distribution of large deletions and inversions at the *LAMA3* locus regardless of whether DSBs were induced by Cas9-g5, Cas9-g6, or Cas9n-g5+6 (Figure 4E). The number of on-target aberration reads was highest in Cas9-g6-edited samples (around 50%) and displayed the longest mean deletion length (Figures 4E and 4F), which was confirmed by Nanopore long-read sequencing of the *LAMA3* target site (Figures 4G and S4E; Table S5). In line with the previous data of the *COL7A1* and *COL17A1* loci, a large proportion of insertions was detected in the double-nickase-edited sample by long-read sequencing (Figure 4G; Table S5), and the SIQ PlotteR analysis confirmed an increased fraction of tandem duplications and templated insertions in Cas9n-g5+6-edited samples when compared to nuclease-treated cells (Figure S4F).

In toto, our results indicate that the extent of on-target aberrations is highly dependent on the genome-editing modality that is used to edit a target locus. While single nicks leave little damage to the genome, the creation of DSBs by nucleases or paired nickases inevitably leads to genomic structural variations in a substantial fraction of target alleles. Notably, a staggered DSB appears to alter the quality of DNA repair, resulting in more templated insertions at all three loci.

DISCUSSION

We show here for the first time a comprehensive genome-wide analysis of chromosomal aberrations that are associated with CRISPR-Cas9 double-nickase-based editing in clinically relevant human cells. Targeting three EB-causing mutations in three different genomic loci (*COL7A1*, *COL17A1*, *LAMA3*) in three EB patient-derived primary keratinocytes, our data demonstrate that frequent and prominent chromosomal rearrangements induced by off-target editing of Cas9 nucleases are eliminated when the same gRNAs were combined in paired-Cas9n approaches. Of note, allelic on-target editing frequencies with the paired-nickase strategy reached over 90% at all three loci and was on par with the respective CRISPR-Cas9 nuclease approaches. The excellent safety profile of paired-nickase editing is based on the fact that single off-target nicks are repaired by precise BER[35] and are not prone to trigger chromosomal translocations, which are mostly mediated by classical NHEJ[26,37,42] but can also form as a result of alt-NHEJ pathways.[10,47] For example, while the fraction of indels at identified off-targets in Cas9-nuclease-edited cells reached up to 93%, the corresponding nickases caused almost no indels at the same sites and did not elicit any detectable translocations.

On the other hand, on-target aberrations, such as large deletions and inversions, have been a hallmark of the genotoxicity profile of a designer nuclease. Although we observed target-locus-specific differences, it is safe to postulate that all DSB-inducing agents, including paired nickases, induce substantial on-target aberrations, the extent of which is locus and target specific. This is consistent with the observations in a previous study investigating large deletions as a result of Cas9 nuclease or Cas9 double-nickase editing using a ddPCR approach.[48] Large deletions at the on-target site have been shown to arise from the alt-NHEJ microhomology-mediated end-joining pathway, in particular TMEJ.[47–50] As described before,[46] our analysis of double-nickase-edited cells confirmed an increase in the frequency of templated insertions, a hallmark of TMEJ repair.[51] An increase in TMEJ after double-nickase editing could thus favor the formation of large deletions, which could possibly be prevented by the use of small-molecule inhibitors of Pol θ.[50,52] Of note, double-nickase-edited cells also displayed an increased number of 5′ overhang fill in or tandem duplications, which are a repair result of DNA breaks with protruding ends[53] and are unlikely to contribute to larger-scale on-target rearrangements. Notably, the presence of an ssODN repair template had little effect on the extent of chromosomal aberrations induced by the dual-nickase approach. The reasons for this remain unclear and should be addressed in future studies.

On-target aberrations are directly detected and visualized by CAST-seq, giving the advantage of looking at on-target and off-target effects

Figure 4. On-target and OT effects of paired nickases targeting *LAMA3*

(A) Schematic representation of the *LAMA3* locus on chromosome 18. Positions of the two gRNAs are highlighted in blue, the PAM in purple, and the cleavage sites by red triangles. Patient-specific mutation c.466_467delCA is shown in red with an asterisk. (B) Chromosomal rearrangements. Circos plots summarize the CAST-seq results of single-nuclease- or double-nickase-edited cells. Aberrations at the on-target site are indicated in green, while the OMT is displayed in red. (C and D) OT activity. Shown is the chromosomal coordinate of the nominated OT site for Cas9-g5, the number of CAST-Seq hits, and the alignment to the on-target site (C), as well as the fraction of indels detected at the nominated OT using NGS (D). (E) Chromosomal aberrations at the on-target site. The CAST-seq coverage plots show all reads mapped to a ±10 kb region around the *LAMA3* target site. The sequencing direction of the bait primer is indicated by a black arrow. The x axis indicates the chromosomal coordinates, the y axis the log2 read CPM, and the dotted line the cleavage site. DELs are shown in orange and INVs in purple. (F) Quantification of CAST-seq coverage. The percentage of large chromosomal aberrations was calculated as the fraction of CAST-seq reads within a ±10 kb window around the cleavage site that were more than 200 bp away from the target site. The mean DEL lengths were calculated within a ±10 kb window around the target site. (G) Quantification of long-read sequencing. Reads of indicated samples were classified into differently sized DELs or insertions. ssODN indicates the presence of a repair template.

with the same assay. This will facilitate the identification of safe genome-editing tools in terms of both reduced off-target activity as well as minimal on-target aberrations. We demonstrated that a large fraction (up to 50%) of aberrations at the on-target site exceed a size of ±200 bp around the cleavage site, which would be missed by standard NGS-based short-read sequencing. Of note, one limitation of CAST-seq is that large deletions at the on-target site cannot be distinguished from templated insertions due to the short sequencing length. Some of the reads that were classified as large deletions could therefore stem from templated insertions, which were particularly highly present in the paired-nickase samples. However, the long-read sequencing data overall confirmed the CAST-seq/D-CAST data, in particular the high number of large deletions that are also present in the paired-nickase sample. CAST-seq is therefore well suited to compare on-target aberrations caused by different editing modalities or different gRNAs targeting the same locus.

The genome-wide analysis presented here using CAST-seq entails several distinct advantages over previous analyses that investigated nickase-induced off-target editing and translocations. Even though different lines of research have demonstrated reduced off-target indel formation and chromosomal aberrations when using nickases, the majority of these studies were conducted in transformed cell lines such as HEK293T,[26,34] K562,[38] or HeLa[38] cells, all of which harbor anomalous karyotypes and altered DNA damage sensing and repair mechanisms. Furthermore, previous studies almost exclusively focused on investigating predicted or already known off-target sites rather than searching for off-targets in an unbiased and genome-wide manner.[34,38–41] When HTGTS was used in HEK293T cells and induced pluripotent stem cells as a first genome-wide assessment of nickase-induced large-scale chromosomal rearrangements, no translocations to off-target sites were identified in single- or double-Cas9n approaches.[22–25,37] As opposed to comparable assays, CAST-seq has proven to be highly sensitive, detecting one chromosomal aberration in 10,000 cells.[22] And, in contrast to HTGTS, CAST-seq is performed with only 500 ng of input genomic DNA for each analysis (25 μg for HTGTS), making it amenable to the analysis of precious primary patient material or post-treatment follow-up.

Compared to previous *in silico* off-target prediction and *in vitro* off-target assays used to characterize the specificity of the employed gRNAs for *COL7A1* and *COL17A1*, the strategy described in this study was more sensitive and more specific in identifying off-target effects in that it detected a higher number of off-target sites and all but one of them could be confirmed. Of note, CAST-seq has a sensitivity of detecting 1 chromosomal rearrangement in 10,000 cells, which is 10-fold higher than the 0.1% detection limit of NGS-based amplicon sequencing. This may explain why no indels were detected at the predicted off-target site for *LAMA3* Cas9-g5, although the translocation that was identified by CAST-seq could be confirmed via direct PCR with chromosomal fusion precisely at the predicted cleavage sites.

In order to assign detected off-target effects to one or the two gRNAs used in paired-nickase approaches, the D-CAST pipeline was developed and is available for use along with the original CAST-seq[22] and T-CAST[23] pipelines. D-CAST not only allows for the simultaneous use of two gRNAs (either two nickases or two nucleases) but also incorporates some of the improvements that were developed for T-CAST, such as improved prediction of the off-target editing site. In conclusion, given that double-nickase editing is equally efficient at gene disruption and, when combined with a template for homologous recombination, can result in similar or higher HDR frequencies compared to nuclease-based editing,[44,54–56] this safe strategy represents an attractive alternative to CRISPR-Cas9-based genome editing, especially in situations where target- or mutation-specific constraints prevent the design of highly specific gRNAs.

MATERIALS AND METHODS

Patient-derived keratinocytes

For the generation of primary cell lines, tissue samples were obtained upon written informed consent at the Department of Dermatology and Allergology, University Hospital Salzburg. Ethical approval was granted by the ethics committee of the county of Salzburg (vote numbers: 415-E/2118/9-2017 and 415-E/2118/43-2023). All procedures described in this study are in full accordance with Austrian legislation and with the Declaration of Helsinki. No animals were used in this study.

For the enzymatic separation of the epidermis from the dermis, the skin biopsies (3–8 mm) were incubated on a shaker overnight at 4°C in CNT-PRIME medium (CELLnTEC) supplemented with 1× Dispase II (Roche, 100× Stock solution = 250 mg in 50 mL PBS). After separation of the two skin layers, the epidermis was floated on top of a drop of a 1× trypsin/EDTA solution (Sigma-Aldrich) for enzymatic isolation of human keratinocytes. After inactivation with chelaxed hyClone calf serum (Thermo Scientific, Waltham, MA, USA) diluted (1:10) in PBS, the cells were pelleted at 200 g for 5 min at room temperature and seeded into collagen I (Sigma-Aldrich) precoated cell culture plates. Primary RDEB and JEB keratinocytes were cultivated in CNT-PRIME medium supplemented with 50 mg/mL Primocin (InvivoGen) and maintained at 37°C and 5% carbon dioxide in a humidified incubator.

Oligonucleotides and gRNAs

All gRNA sequences, primers for CAST-seq, primers for NGS-based amplicon sequencing, and primers for long-read nanopore sequencing are listed in Table S7. The gRNAs were ordered from Integrated DNA Technologies (IDT). ssODN sequences are listed in Table S6.

Electroporation

Electroporation of RNPs into keratinocytes was performed using the Neon transfection system (Thermo Scientific) under the following conditions: 1,400 V, 20 ms, 2 pulses. 250,000 cells were treated with Alt-R SpCas9 Nuclease V3 or Alt-R SpCas9 D10A Nickase V3 (IDT) together with the gRNA (IDT) at a ratio of 4:1 (3 μg + 750 ng). In indicated experiments, 250 ng ssODN was added to the

electroporation reaction. Genomic DNA from RNP-treated keratinocytes was isolated 1 week post-transfection.

CAST-seq analysis

Genomic DNA was extracted using the ReliaPrep Blood gDNA Miniprep System kit (Promega) according to the manufacturer's protocol. CAST-seq analyses were performed as previously described[22] but with the following modifications: enzymatic fragmentation of the genomic DNA was aimed at an average length of 500 bp. CAST-seq libraries were sequenced on a NovaSeq 6000 using 2× 150 bp paired-end sequencing (GENEWIZ, Azenta Life Sciences). For each sample, two technical replicates were run and analyzed. Only sites that were detected as significant hits in both technical replicates were further analyzed by targeted amplicon sequencing. CAST-seq results are provided in Tables S1 (*COL7A1* samples), S2 (*COL17A1*), and S3 (*LAMA3*).

The CAST-seq bioinformatic pipeline was adjusted for the simultaneous use of two gRNAs. Each spacer sequence was separately aligned to the putative sites, and therefore each spacer received its own score and p value derived from an empirical cumulative distribution function on random sequences. Sites under investigation were labeled as OMT if any of the two p values reached the cutoff of 0.005 (vs. 0.05 previously used[22] to reduce false positive OMTs). The definitions of HMT and NBS were not affected by the use of the two gRNAs. Further adjustments to the CAST-seq algorithm include barcode hopping annotation and coverage analysis to speed up the execution time by aligning the gRNAs only to the most covered regions for each site, as described for T-CAST.[23]

CAST-seq read coverage was plotted as follows: the ±10 kb window around the on-target site was divided into bins of 100 bp, and all reads falling in a respective bin were displayed as log2 read counts per million. Quantifications of the CAST-seq coverage plots were calculated the following way: % large aberrations = sum of all reads in bins >200 bp from the cleavage site/sum of all reads in all bins. Mean deletion length = sum of (count of deletion reads * distance from the cleavage site)/sum of all deletion reads. Deletion reads are all negative or positive reads depending on the CAST-seq read orientation.

Short-read sequencing

80 ng genomic DNA was used as a template for amplification via a 30 cycle PCR using Q5 Hot Start High-Fidelity DNA Polymerase (New England Biolabs [NEB]) using primers listed in Table S7. PCR fragments were purified using the QIAquick PCR Purification Kit (-QIAGEN), subjected to Sanger sequencing (Eurofins Genomics), and analyzed using DECODR.[57] Alternatively, purified PCR products were pooled and prepared for NGS using the NEBNext Ultra II DNA Library Prep Kit for Illumina (NEB) and sequenced on Illumina HiSeq or NovaSeq platforms with 2 × 150 bp read length (GENEWIZ, Azenta Life Sciences). Reads were analyzed using the CRISPResso2 package[58] with the following settings: window of 20 around the cleavage site, quality 30, ignoring substitutions. For double-nickase-edited samples, a window of 40 was set around the middle of the two cleavage sites. In one case (Figure 3D, OT1*), insertions were ignored due to a minor amplification of an unspecific fragment. Significance was determined using CRISPResso Compare.

Long-read sequencing

A 5 kb amplicon spanning the *COL7A1* target site was amplified from 200 ng genomic DNA by a 30 cycle PCR using KAPA HiFi HotStart PCR Kit (Roche) using primers listed in Table S7. PCR fragments were purified using AMPure XP beads (Beckman Coulter) at a 1.8:1 bead-to-sample ratio. Libraries were prepared using the Nanopore Ligation Sequencing Kit V14 (SQK-LSK114) (*COL7A1*) or the Native Barcoding Kit 24 V14 (SQK-NBD114.24) (*COL7A1*+ssODN, *COL17A1*±ssODN, *LAMA3*) according to the manufacturer's protocol and sequenced on a MinION Flow Cell. Reads were demultiplexed by employing a custom pipeline that allows up to 4 mismatches in the barcode sequence.[59] Obtained reads were aligned using Minimap2 v.2.24-r1122[60] and further processed with SAMtools.[61] Deletions and insertions were counted from the cigar string in a window of 200 bp around the cleavage site using a custom script. Deletion read coverage was calculated by subtracting the read coverage with deletions from the read coverage without the deletions and by normalizing the reads to the total reads for each sample. The values obtained from the untreated control were subtracted from the treated samples to decrease sequencing bias. Insertion sequences were extracted from the SAM file and aligned to the reference amplicon using a BLAST-like algorithm (LAST v.1411).[62]

Translocation PCR

50 ng genomic DNA was used as input for a 50 cycle PCR using Q5 Hot Start High-Fidelity DNA Polymerase (NEB) employing primers listed in Table S7. The amplified product was gel purified using the QIAquick Gel Extraction Kit (QIAGEN), sent for Sanger sequencing (Eurofins Genomics), and aligned to *LAMA3* and OT1 using SnapGene (Dotmatics).

DATA AND CODE AVAILABILITY

Data generated or analyzed during this study are included in this article and its supplemental data files. The D-CAST code is available on GitHub (https://github.com/AG-Boerries/CAST-Seq). Raw data were deposited in the Gene Expression Omnibus repository and are publicly available under the accession number GEO: GSE241780.

SUPPLEMENTAL INFORMATION

Supplemental information can be found online at https://doi.org/10.1016/j.ymthe.2024.03.006.

ACKNOWLEDGMENTS

We thank Giandomenico Turchiano for support with the CAST-seq setup, Claudio Mussolino for critical conversations and support, and the members of our laboratories for constructive discussions and suggestions. This work was supported by the German Research Foundation (DFG) to T.C. (CA 311/4-1 and FANEDIT/EJPRD20-209) and M.B. (CRC 1160, project 256073931-Z02), DEBRA Austria to U.K., T.K.,

and S.H., the LHF Charitable Trust (LHFCT) to J.B., and the German Federal Ministry of Education and Research (BMBF) to T.I.C. and T.C. (editCCR5–01EK2205), M.B. (MIRACUM-01ZZ1801B), and G.A. (EkoEstMed–01ZZ2015). Figures 1A, 3A, 4A, S1A, S1C, S3B, and S4B were created with BioRender.com.

AUTHOR CONTRIBUTIONS

T.C., U.K., T.K., T.I.C., and M.B. supervised the project and acquired funding. J.K., M.R., T.K., U.K., and T.C. conceived and designed the experiments. J.K., M.R., T.K., K.O.C., J.B., S.H., and M.e.G. performed the experiments. J.K., M.R., K.O.C., and G.A. analyzed the data. K.O.C. and G.A. developed software. J.K., M.R., and T.C. wrote the first draft of the paper. All authors reviewed and edited the paper.

DECLARATION OF INTERESTS

T.C. is an advisor to Cimeio Therapeutics, Excision BioTherapeutics, GenCC, and Novo Nordisk. T.C. and T.I.C. have sponsored research collaborations with Cellectis and Cimeio Therapeutics, respectively. T.C., M.B., and G.A. hold a patent on CAST-seq (US11319580B2).

DECLARATION OF GENERATIVE AI AND AI-ASSISTED TECHNOLOGIES IN THE WRITING PROCESS

During the preparation of this work, the authors used AI-assisted technologies (DeepL) to improve readability and language. The authors reviewed and edited the content after using these tools as needed and take full responsibility for the content of the publication.

REFERENCES

1. Bailey, S.R., and Maus, M.V. (2019). Gene editing for immune cell therapies. Nat. Biotechnol. *37*, 1425–1434.
2. Cornu, T.I., Mussolino, C., and Cathomen, T. (2017). Refining strategies to translate genome editing to the clinic. Nat. Med. *23*, 415–423.
3. Zarghamian, P., Klermund, J., and Cathomen, T. (2022). Clinical genome editing to treat sickle cell disease-A brief update. Front. Med. (Lausanne) *9*, 1065377.
4. Gasiunas, G., Barrangou, R., Horvath, P., and Siksnys, V. (2012). Cas9-crRNA ribonucleoprotein complex mediates specific DNA cleavage for adaptive immunity in bacteria. Proc. Natl. Acad. Sci. USA *109*, E2579–E2586.
5. Jinek, M., Chylinski, K., Fonfara, I., Hauer, M., Doudna, J.A., and Charpentier, E. (2012). A programmable dual-RNA-guided DNA endonuclease in adaptive bacterial immunity. Science *337*, 816–821.
6. Fu, Y., Foden, J.A., Khayter, C., Maeder, M.L., Reyon, D., Joung, J.K., and Sander, J.D. (2013). High-frequency off-target mutagenesis induced by CRISPR-Cas nucleases in human cells. Nat. Biotechnol. *31*, 822–826.
7. Hsu, P.D., Scott, D.A., Weinstein, J.A., Ran, F.A., Konermann, S., Agarwala, V., Li, Y., Fine, E.J., Wu, X., Shalem, O., et al. (2013). DNA targeting specificity of RNA-guided Cas9 nucleases. Nat. Biotechnol. *31*, 827–832.
8. Chang, H.H.Y., Pannunzio, N.R., Adachi, N., and Lieber, M.R. (2017). Non-homologous DNA end joining and alternative pathways to double-strand break repair. Nat. Rev. Mol. Cell Biol. *18*, 495–506.
9. Ramsden, D.A., Carvajal-Garcia, J., and Gupta, G.P. (2022). Mechanism, cellular functions and cancer roles of polymerase-theta-mediated DNA end joining. Nat. Rev. Mol. Cell Biol. *23*, 125–140.
10. Mateos-Gomez, P.A., Gong, F., Nair, N., Miller, K.M., Lazzerini-Denchi, E., and Sfeir, A. (2015). Mammalian polymerase theta promotes alternative NHEJ and suppresses recombination. Nature *518*, 254–257.
11. Fichter, K.M., Setayesh, T., and Malik, P. (2023). Strategies for precise gene edits in mammalian cells. Mol. Ther. Nucleic Acids *32*, 536–552.
12. Scully, R., Panday, A., Elango, R., and Willis, N.A. (2019). DNA double-strand break repair-pathway choice in somatic mammalian cells. Nat. Rev. Mol. Cell Biol. *20*, 698–714.
13. Bae, S., Park, J., and Kim, J.S. (2014). Cas-OFFinder: a fast and versatile algorithm that searches for potential off-target sites of Cas9 RNA-guided endonucleases. Bioinformatics *30*, 1473–1475.
14. Cradick, T.J., Qiu, P., Lee, C.M., Fine, E.J., and Bao, G. (2014). COSMID: A Web-based Tool for Identifying and Validating CRISPR/Cas Off-target Sites. Mol. Ther. Nucleic Acids *3*, e214.
15. Cancellieri, S., Zeng, J., Lin, L.Y., Tognon, M., Nguyen, M.A., Lin, J., Bombieri, N., Maitland, S.A., Ciuculescu, M.F., Katta, V., et al. (2023). Human genetic diversity alters off-target outcomes of therapeutic gene editing. Nat. Genet. *55*, 34–43.
16. Tsai, S.Q., Nguyen, N.T., Malagon-Lopez, J., Topkar, V.V., Aryee, M.J., and Joung, J.K. (2017). CIRCLE-seq: a highly sensitive in vitro screen for genome-wide CRISPR-Cas9 nuclease off-targets. Nat. Methods *14*, 607–614.
17. Lazzarotto, C.R., Malinin, N.L., Li, Y., Zhang, R., Yang, Y., Lee, G., Cowley, E., He, Y., Lan, X., Jividen, K., et al. (2020). CHANGE-seq reveals genetic and epigenetic effects on CRISPR-Cas9 genome-wide activity. Nat. Biotechnol. *38*, 1317–1327.
18. Tsai, S.Q., Zheng, Z., Nguyen, N.T., Liebers, M., Topkar, V.V., Thapar, V., Wyvekens, N., Khayter, C., Iafrate, A.J., Le, L.P., et al. (2015). GUIDE-seq enables genome-wide profiling of off-target cleavage by CRISPR-Cas nucleases. Nat. Biotechnol. *33*, 187–197.
19. Wienert, B., Wyman, S.K., Richardson, C.D., Yeh, C.D., Akcakaya, P., Porritt, M.J., Morlock, M., Vu, J.T., Kazane, K.R., Watry, H.L., et al. (2019). Unbiased detection of CRISPR off-targets in vivo using DISCOVER-Seq. Science *364*, 286–289.
20. Korablev, A., Lukyanchikova, V., Serova, I., and Battulin, N. (2020). On-Target CRISPR/Cas9 Activity Can Cause Undesigned Large Deletion in Mouse Zygotes. Int. J. Mol. Sci. *21*, 3604.
21. Kosicki, M., Tomberg, K., and Bradley, A. (2018). Repair of double-strand breaks induced by CRISPR-Cas9 leads to large deletions and complex rearrangements. Nat. Biotechnol. *36*, 765–771.
22. Turchiano, G., Andrieux, G., Klermund, J., Blattner, G., Pennucci, V., El Gaz, M., Monaco, G., Poddar, S., Mussolino, C., Cornu, T.I., et al. (2021). Quantitative evaluation of chromosomal rearrangements in gene-edited human stem cells by CAST-Seq. Cell Stem Cell *28*, 1136–1147.e5.
23. Rhiel, M., Geiger, K., Andrieux, G., Rositzka, J., Boerries, M., Cathomen, T., and Cornu, T.I. (2023). T-CAST: An optimized CAST-Seq pipeline for TALEN confirms superior safety and efficacy of obligate-heterodimeric scaffolds. Front. Genome Ed. *5*, 1130736.
24. Frock, R.L., Hu, J., Meyers, R.M., Ho, Y.J., Kii, E., and Alt, F.W. (2015). Genome-wide detection of DNA double-stranded breaks induced by engineered nucleases. Nat. Biotechnol. *33*, 179–186.
25. Hu, J., Meyers, R.M., Dong, J., Panchakshari, R.A., Alt, F.W., and Frock, R.L. (2016). Detecting DNA double-stranded breaks in mammalian genomes by linear amplification-mediated high-throughput genome-wide translocation sequencing. Nat. Protoc. *11*, 853–871.
26. Cullot, G., Boutin, J., Toutain, J., Prat, F., Pennamen, P., Rooryck, C., Teichmann, M., Rousseau, E., Lamrissi-Garcia, I., Guyonnet-Duperat, V., et al. (2019). CRISPR-Cas9 genome editing induces megabase-scale chromosomal truncations. Nat. Commun. *10*, 1136.
27. Nahmad, A.D., Reuveni, E., Goldschmidt, E., Tenne, T., Liberman, M., Horovitz-Fried, M., Khosravi, R., Kobo, H., Reinstein, E., Madi, A., et al. (2022). Frequent aneuploidy in primary human T cells after CRISPR-Cas9 cleavage. Nat. Biotechnol. *40*, 1807–1813.
28. Boutin, J., Rosier, J., Cappellen, D., Prat, F., Toutain, J., Pennamen, P., Bouron, J., Rooryck, C., Merlio, J.P., Lamrissi-Garcia, I., et al. (2021). CRISPR-Cas9 globin editing can induce megabase-scale copy-neutral losses of heterozygosity in hematopoietic cells. Nat. Commun. *12*, 4922.
29. Leibowitz, M.L., Papathanasiou, S., Doerfler, P.A., Blaine, L.J., Sun, L., Yao, Y., Zhang, C.Z., Weiss, M.J., and Pellman, D. (2021). Chromothripsis as an on-target consequence of CRISPR-Cas9 genome editing. Nat. Genet. *53*, 895–905.

30. Liu, Y., Yin, J., Gan, T., Liu, M., Xin, C., Zhang, W., and Hu, J. (2022). PEM-seq comprehensively quantifies DNA repair outcomes during gene-editing and DSB repair. STAR Protoc. *3*, 101088.

31. Yin, J., Liu, M., Liu, Y., Wu, J., Gan, T., Zhang, W., Li, Y., Zhou, Y., and Hu, J. (2019). Optimizing genome editing strategy by primer-extension-mediated sequencing. Cell Discov. *5*, 18.

32. Cong, L., Ran, F.A., Cox, D., Lin, S., Barretto, R., Habib, N., Hsu, P.D., Wu, X., Jiang, W., Marraffini, L.A., and Zhang, F. (2013). Multiplex genome engineering using CRISPR/Cas systems. Science *339*, 819–823.

33. Mali, P., Aach, J., Stranges, P.B., Esvelt, K.M., Moosburner, M., Kosuri, S., Yang, L., and Church, G.M. (2013). CAS9 transcriptional activators for target specificity screening and paired nickases for cooperative genome engineering. Nat. Biotechnol. *31*, 833–838.

34. Ran, F.A., Hsu, P.D., Lin, C.Y., Gootenberg, J.S., Konermann, S., Trevino, A.E., Scott, D.A., Inoue, A., Matoba, S., Zhang, Y., and Zhang, F. (2013). Double nicking by RNA-guided CRISPR Cas9 for enhanced genome editing specificity. Cell *154*, 1380–1389.

35. Dianov, G.L., and Hübscher, U. (2013). Mammalian base excision repair: the forgotten archangel. Nucleic Acids Res. *41*, 3483–3490.

36. Kuzminov, A. (2001). Single-strand interruptions in replicating chromosomes cause double-strand breaks. Proc. Natl. Acad. Sci. USA *98*, 8241–8246.

37. Chen, X., Tasca, F., Wang, Q., Liu, J., Janssen, J.M., Brescia, M.D., Bellin, M., Szuhai, K., Kenrick, J., Frock, R.L., and Gonçalves, M.A.F.V. (2020). Expanding the editable genome and CRISPR-Cas9 versatility using DNA cutting-free gene targeting based on in trans paired nicking. Nucleic Acids Res. *48*, 974–995.

38. Cho, S.W., Kim, S., Kim, Y., Kweon, J., Kim, H.S., Bae, S., and Kim, J.S. (2014). Analysis of off-target effects of CRISPR/Cas-derived RNA-guided endonucleases and nickases. Genome Res. *24*, 132–141.

39. Shen, B., Zhang, W., Zhang, J., Zhou, J., Wang, J., Chen, L., Wang, L., Hodgkins, A., Iyer, V., Huang, X., and Skarnes, W.C. (2014). Efficient genome modification by CRISPR-Cas9 nickase with minimal off-target effects. Nat. Methods *11*, 399–402.

40. Bischof, J., March, O.P., Liemberger, B., Haas, S.A., Hainzl, S., Petković, I., Leb-Reichl, V., Illmer, J., Korotchenko, E., Klausegger, A., et al. (2022). Paired nicking-mediated COL17A1 reframing for junctional epidermolysis bullosa. Mol. Ther. *30*, 2680–2692.

41. Kocher, T., Wagner, R.N., Klausegger, A., Guttmann-Gruber, C., Hainzl, S., Bauer, J.W., Reichelt, J., and Koller, U. (2019). Improved Double-Nicking Strategies for COL7A1-Editing by Homologous Recombination. Mol. Ther. Nucleic Acids *18*, 496–507.

42. Ghezraoui, H., Piganeau, M., Renouf, B., Renaud, J.B., Sallmyr, A., Ruis, B., Oh, S., Tomkinson, A.E., Hendrickson, E.A., Giovannangeli, C., et al. (2014). Chromosomal translocations in human cells are generated by canonical nonhomologous end-joining. Mol. Cell *55*, 829–842.

43. Bardhan, A., Bruckner-Tuderman, L., Chapple, I.L.C., Fine, J.D., Harper, N., Has, C., Magin, T.M., Marinkovich, M.P., Marshall, J.F., McGrath, J.A., et al. (2020). Epidermolysis bullosa. Nat. Rev. Dis. Primers *6*, 78.

44. Kocher, T., Bischof, J., Haas, S.A., March, O.P., Liemberger, B., Hainzl, S., Illmer, J., Hoog, A., Muigg, K., Binder, H.M., et al. (2021). A non-viral and selection-free COL7A1 HDR approach with improved safety profile for dystrophic epidermolysis bullosa. Mol. Ther. Nucleic Acids *25*, 237–250.

45. Petković, I., Bischof, J., Kocher, T., March, O.P., Liemberger, B., Hainzl, S., Strunk, D., Raninger, A.M., Binder, H.M., Reichelt, J., et al. (2022). COL17A1 editing via homology-directed repair in junctional epidermolysis bullosa. Front. Med. (Lausanne) *9*, 976604.

46. van Schendel, R., Schimmel, J., and Tijsterman, M. (2022). SIQ: easy quantitative measurement of mutation profiles in sequencing data. NAR Genom. Bioinform. *4*, lqac063.

47. McVey, M., and Lee, S.E. (2008). MMEJ repair of double-strand breaks (director's cut): deleted sequences and alternative endings. Trends Genet. *24*, 529–538.

48. Owens, D.D.G., Caulder, A., Frontera, V., Harman, J.R., Allan, A.J., Bucakci, A., Greder, L., Codner, G.F., Hublitz, P., McHugh, P.J., et al. (2019). Microhomologies are prevalent at Cas9-induced larger deletions. Nucleic Acids Res. *47*, 7402–7417.

49. Kosicki, M., Allen, F., Steward, F., Tomberg, K., Pan, Y., and Bradley, A. (2022). Cas9-induced large deletions and small indels are controlled in a convergent fashion. Nat. Commun. *13*, 3422.

50. Schimmel, J., Muñoz-Subirana, N., Kool, H., van Schendel, R., van der Vlies, S., Kamp, J.A., de Vrij, F.M.S., Kushner, S.A., Smith, G.C.M., Boulton, S.J., and Tijsterman, M. (2023). Modulating mutational outcomes and improving precise gene editing at CRISPR-Cas9-induced breaks by chemical inhibition of end-joining pathways. Cell Rep. *42*, 112019.

51. Schimmel, J., van Schendel, R., den Dunnen, J.T., and Tijsterman, M. (2019). Templated Insertions: A Smoking Gun for Polymerase Theta-Mediated End Joining. Trends Genet. *35*, 632–644.

52. Wimberger, S., Akrap, N., Firth, M., Brengdahl, J., Engberg, S., Schwinn, M.K., Slater, M.R., Lundin, A., Hsieh, P.P., Li, S., et al. (2023). Simultaneous inhibition of DNA-PK and Polθ improves integration efficiency and precision of genome editing. Nat. Commun. *14*, 4761.

53. Schiml, S., Fauser, F., and Puchta, H. (2016). Repair of adjacent single-strand breaks is often accompanied by the formation of tandem sequence duplications in plant genomes. Proc. Natl. Acad. Sci. USA *113*, 7266–7271.

54. Bothmer, A., Phadke, T., Barrera, L.A., Margulies, C.M., Lee, C.S., Buquicchio, F., Moss, S., Abdulkerim, H.S., Selleck, W., Jayaram, H., et al. (2017). Characterization of the interplay between DNA repair and CRISPR/Cas9-induced DNA lesions at an endogenous locus. Nat. Commun. *8*, 13905.

55. Gopalappa, R., Suresh, B., Ramakrishna, S., and Kim, H.H. (2018). Paired D10A Cas9 nickases are sometimes more efficient than individual nucleases for gene disruption. Nucleic Acids Res. *46*, e71.

56. Vriend, L.E.M., Prakash, R., Chen, C.C., Vanoli, F., Cavallo, F., Zhang, Y., Jasin, M., and Krawczyk, P.M. (2016). Distinct genetic control of homologous recombination repair of Cas9-induced double-strand breaks, nicks and paired nicks. Nucleic Acids Res. *44*, 5204–5217.

57. Bloh, K., Kanchana, R., Bialk, P., Banas, K., Zhang, Z., Yoo, B.C., and Kmiec, E.B. (2021). Deconvolution of Complex DNA Repair (DECODR): Establishing a Novel Deconvolution Algorithm for Comprehensive Analysis of CRISPR-Edited Sanger Sequencing Data. CRISPR J. *4*, 120–131.

58. Clement, K., Rees, H., Canver, M.C., Gehrke, J.M., Farouni, R., Hsu, J.Y., Cole, M.A., Liu, D.R., Joung, J.K., Bauer, D.E., and Pinello, L. (2019). CRISPResso2 provides accurate and rapid genome editing sequence analysis. Nat. Biotechnol. *37*, 224–226.

59. Tange, O. (2018). GNU Parallel 2018 (Lulu. com).

60. Li, H. (2018). Minimap2: pairwise alignment for nucleotide sequences. Bioinformatics *34*, 3094–3100.

61. Danecek, P., Bonfield, J.K., Liddle, J., Marshall, J., Ohan, V., Pollard, M.O., Whitwham, A., Keane, T., McCarthy, S.A., Davies, R.M., and Li, H. (2021). Twelve years of SAMtools and BCFtools. Gigascience *10*, giab008.

62. Kiełbasa, S.M., Wan, R., Sato, K., Horton, P., and Frith, M.C. (2011). Adaptive seeds tame genomic sequence comparison. Genome Res. *21*, 487–493.